Kinetic Study of the Oxidation of Pyrite in Aqueous Ferric Sulfate

Chang Qiong Zheng,[†] Charles C. Allen,[‡] and Renato G. Bautista*[§]

Ames Laboratory USDOE, Mining and Mineral Resources Research Institute and Department of Chemical Engineering, Iowa State University, Ames, Iowa 50011

The oxidation of pyrite in aqueous ferric sulfate is given by the chemical reaction $FeS_2 + 14Fe^{3+} + 8H_2O \rightarrow 15Fe^{2+} + 2SO_4^{2-} + 16H^+$. It was found that the reaction was kinetically limited and the oxidation rate for the pyrite depended on the total iron concentration and on the ratio of ferric to ferrous ions under constant acid concentration. The experimental data were found to best fit the Hougen–Watson dual-site adsorption model for total Fe(III) and total Fe(II) ions with the rate expression given by

$$r_{FeS_2} = \frac{k_1 - k_2[Fe(II)]^{1/2}[Fe(III)]^{1/2}}{1/[Fe(III)]^{1/2} + k_3 + k_4[Fe(II)/Fe(III)]^{1/2}}$$

It was also found that the rate of pyrite oxidation depended on the free ferric, free ferrous, and bisulfate ions when the sulfate concentration is varied. The experimental data could be represented by a Hougen–Watson simple adsorption–irreversible reaction model for Fe^{3+}, Fe^{2+}, and HSO_4^- ions with the rate expression given by eq 65.

Acidified ferric ion solution is an effective lixiviant for many metals from low-grade sulfide or oxide ores that are leached by dump, heap, or in situ methods. Usually, the ferric ion leaching medium can be generated from the pyrite present with the valuable mineral in the ore. The results of studies on the rate and the reaction mechanism of pyrite oxidation by ferric ion solution is therefore of importance in hydrometallurgical processing.

Recently Lowson (1982) reviewed the aqueous oxidation of pyrite by molecular oxygen listing a large number of references, part of which described the oxidation of pyrite by ferric ion. Lowson reported that three reaction paths have been identified for the aqueous oxidation of pyrite by molecular oxygen, namely, bacterial, chemical, and electrochemical. Bacterial and electrochemical paths will not be discussed in detail in this paper.

Early work on the bacterial leaching of pyrite showed that there were two mechanisms in effect: indirect leaching and direct leaching. Braley (1953), Sutton and Corrick (1963, 1964), Corrick and Sutton (1965), and Smith and Shumate (1970) noted that the role of the bacteria was to catalyze the oxidation of ferrous ions to ferric ions in solution by the reaction

$$4Fe^{2+} + 4H^+ + O_2 \xrightarrow{\text{bacteria}} 4Fe^{3+} + 2H_2O \quad (1)$$

The ferric ion subsequently oxidized the pyrite to form ferrous and sulfate ions according to reaction (2). Since

$$FeS_2 + 14Fe^{3+} + 8H_2O \rightarrow 15Fe^{2+} + 2SO_4^{2-} + 16H^+ \quad (2)$$

this bacterial oxidation of ferrous ions occurs in solution, there is no contact of the bacteria with the pyrite. This mechanism will be referred to as the indirect mechanism.

Other workers, Bryner and Jameson (1958), Schaeffer et al. (1963), and Woodcock (1961), showed that the bacteria adsorbed on the pyrite surface could attack the pyrite, exerting a catalytic effect according to the reaction

$$FeS_2 + {}^7/_2O_2 + H_2O \xrightarrow{\text{bacteria}} Fe^{2+} + 2H^+ + 2SO_4^{2-} \quad (3)$$

Since the bacteria are strict aerobes, the oxygen is required regardless of whether the reactions are of the indirect or direct mechanism. In the present work, the ferric ion is used as the leaching agent for pyrite. The experiments were done in the absence of bacteria and were isolated from air (the N_2 gas was introduced in order to exclude atmospheric O_2). If there were some bacteria in the system, they would be inactive, because of the lack of oxygen. The pyrite oxidation in this research was therefore considered to be due only to the function of ferric ion alone.

The chemical oxidation path is a sequence of three steps: the oxidation of pyrite by molecular oxygen to sulfate and ferrous iron; the oxidation of ferrous by molecular oxygen to ferric iron; and the oxidation of pyrite by ferric iron to sulfate and ferrous iron. The third step which is a heterogeneous surface reaction is of interest in this work. Under normal conditions, the pyrite can be oxidized by ferric ion according to reaction 2 (Stokes, 1970; Garrels and Thompson, 1960; Smith and Shumate, 1970).

The electrochemical oxidation of pyrite by molecular oxygen has been studied by a number of workers (Masuko and Hisamatsu, 1967; Ammou-Chokroum, 1979; Bave and Orlov, 1975; Biegler et al., 1975). The overall process is a summation of cathodic and anodic reactions that are occurring at the pyrite surface.

The anode reaction is

$$FeS_2 + 8H_2O \rightarrow Fe^{3+} + 2SO_4^{2-} + 16H^+ + 15e^- \quad (4)$$

and the cathode reaction is

$$O_2 + 4H^+ + 4e^- \rightarrow 2H_2O \quad (5)$$

The anodic oxidation of pyrite is a complex process, and the mechanism is still not well understood. There is no satisfactory mechanism to explain the oxidation of S^{2-} to SO_4^{2-} and its relation to ferric ion oxidation.

* To whom all correspondence should be addressed.
[†] Visiting chemical engineer at the Ames Laboratory USDOE and is from the Department of Metal Materials, Chengdu University of Science and Technology, Chengdu, Sichuan, People's Republic of China.
[‡] Formerly a graduate assistant at Ames Laboratory USDOE and is now with Honeywell, Minneapolis, MN.
[§] Formerly a group leader and professor at Ames Laboratory USDOE and is now with the Mackay School of Mines, University of Nevada at Reno, Reno, NV 89557.

0196-4305/86/1125-0308$01.50/0

Studies on the oxidation of pyrite by Stokes (1970) indicated that the pyrite could be oxidized by the ferric salt to produce simultaneously both sulfur and sulfate by separate oxidation processes according to reactions 2 and 6 depending on the leaching conditions. Stokes reported that at lower temperatures and higher concentrations of ferric ion, more sulfate was formed.

$$FeS_2 + 2Fe^{3+} \rightarrow 3Fe^{2+} + 2S^0 \quad (6)$$

Garrels and Thompson (1960) studied the leaching of pyrite at 306 K with ferric sulfate solution and showed that under most natural conditions, pyrite was apparently oxidized by ferric ion to ferrous ion, hydrogen ion, and sulfate ion. Oxidation of pyrite by ferric ion only under near equilibrium conditions (at a potential of around 0.250–0.300 V) appears to produce molecular sulfur. Any excess of ferric ions will oxidize this sulfur through intermediate species to sulfate ion.

Smith and Shumate (1970) studied the kinetics of leaching of pyrite by ferric ion solution, at the potential range 0.350–0.600 V and at 298 K. In calculating the rate, the stoichiometry according to eq 2 was found to agree with the theoretical values, within limits of experimental error.

Under the present experimental condition of maintaining the potential values higher than 0.480 V and keeping the temperature at 298 K, the oxidation reaction of pyrite must occur according to eq 2.

Previous kinetic studies reported in the literature (Garrels and Thompson, 1960; Smith and Shumate, 1970; Sasmojo, 1969; King and Pelmutter, 1977; Mathews and Robins, 1972; Lowson, 1977; Allen, 1982) on the oxidation of pyrite using ferric ion solution resulted in diverse rate expressions. The oxidation rate of pyrite was reported to be a function of either the ferric ion concentration and the ferric/ferrous ratio (Smith and Shumate, 1970; Sasmojo, 1969; Allen, 1982), the mole fraction of the ferric ion in the solution (Garrels and Thompson, 1960; Mathews and Robins, 1972), the ferric and ferrous ion concentrations, or the ferric, ferrous, and total iron concentrations (King and Perlmutter, 1977; Lowson, 1979). The effect of sulfate ions on the oxidation rate of pyrite was reported by Sasmojo (1969) and Smith and Shumate (1970) to decrease the oxidation rate of pyrite with increasing sulfate concentration, regardless of whether Na_2SO_4 or H_2SO_4 was used. Mathews and Robins (1972) reported that the rate of oxidation decreased with decreasing pH. Garrels and Thompson (1960) found that there was no change in the oxidation rate when the pH was increased from 0 to 2. In this paper, the kinetics of oxidation of two different pyrite samples in the aqueous solution of ferric sulfate was studied as a function of the total ferric ion concentration Fe(III) and ferric/ferrous ratio, Fe(III)/Fe(II), and as a function of the free ferric, free ferrous, and bisulfate ion concentrations.

Experimental Section

The two pyrite rock samples used in this work were obtained from Sargent-Welch Co. and Foote Mineral Co. (H. Wilhelm sample). The samples were crushed, washed with 6 N H_2SO_4 followed with distilled water, and then dried with acetone or under vacuum. The −60+140 U.S. mesh fraction gave a specific surface area of 128 ± 3 m^2/kg by the BET method. The H. Wilhelm pyrite ore chemical analysis in weight percent was 45.67% iron, 52.08% S, and 97.70% FeS_2. The analytical S to Fe atom ratio was close to the theoretical value for FeS_2. X-ray diffraction analysis showed pyrite was the major constituent and marcasite was present in trace amounts. The electron microprobe analysis showed that FeS_2 is predominant with trace quantities of Cu, Zn, Pb, Si, Al, and Na. No Ni and Cu were detected. In comparison, a typical pyrite concentrate from a copper–zinc–pyrite sulfide ore flotation operation assays 0.121% Cu and 0.74% Zn (Tveter and McQuiston, 1962).

The experimental setup used in this work is similar to that used by Sasmojo (1969) and Allen (1982). It consisted of four main components, a temperature control system sensitive to within ±0.5 °C, a lixiviant circulation system, a packed-bed reactor, and an automatic titration unit. The lixiviant circulation system consists of a rotameter, a peristalic pump, a magnetic stirrer, a continuous-stirred tank reactor (CSTR), and Tygon tubings. The CSTR had a tight-fitting lid with six holes to allow for the insertion of two electrodes, a thermometer, a buret, a sampling port, and an inlet tube for N_2 gas. The N_2 gas was introduced in order to exclude atmospheric O_2. The N_2 gas was saturated with water before being passed into the CSTR in order to keep constant the solution volume. The packed-bed reactor basically consisted of a chamber in which the ore was confined by means of two filter discs. An automatic titration unit was used to maintain constant the leaching solution potential. $KMnO_4$ or $Fe_2(SO_4)_3$ oxidant solution was added in doses of 10^{-2} mL by means of a digital syringe buret controlled by an automatic titrator. The solution pH is measured by a digital pH meter.

The reaction rate was studied as a function of total iron concentration, ferric/ferrous ratio, and total sulfate concentration using H_2SO_4 and/or Na_2SO_4 in the leaching solution.

All the stock solutions were prepared by using analytical grade reagent.

For each run, 0.01 kg of sample was used; 400 mL of leaching solution was prepared by using ferrous sulfate (or ferric sulfate), sulfuric acid, and sodium sulfate. The emf (ferric/ferrous ratio) was set and adjusted by addition of the titrant or by allowing the lixiviant to circulate through the packed-bed reactor until the desired emf was attained.

The rate of $Fe_2(SO_4)_3$ titrant addition was usually so fast that the titrator tended to overshoot the emf setting on the controller. $KMnO_4$ was used instead of $Fe_2(SO_4)_3$ to help alleviate this problem.

The reaction rate for each run was determined from the rate in which the titrant was added to the leaching solution to maintain a constant emf. The overall dissolution reaction occurring in the packed-bed reaction is given by eq 2, while the reaction occurring in the CSTR is given by

$$MnO_4^- + 5Fe^{2+} + 8H^+ \rightarrow Mn^{2+} + 5Fe^{3+} + 4H_2O \quad (7)$$

Since the ferric/ferrous ratio R^* is maintained during the dissolution step,

$$R^* = \frac{Fe^{III}{}_T V_T}{Fe^{II}{}_T V_T} = \frac{Fe^{III}{}_T V_T - 14 r_{FeS_2} m_{FeS_2} t + x}{Fe^{II}{}_T V_T + 15 r_{FeS_2} m_{FeS_2} t - x} \quad (8)$$

Rearranging and solving eq 8 for x yields

$$x = \frac{(15R^* + 14)}{(R^* + 1)} r_{FeS_2} m_{FeS_2} t \quad (9)$$

The rate of Fe(II) oxidation by $KMnO_4$ is thus defined by

$$\frac{dx}{dt} = \frac{(15R^* + 14)}{(R^* + 1)} r_{FeS_2} m_{FeS_2} \quad (10)$$

Substituting into eq 10 the normality of the titrant, N, and the rate of titrant addition, υ (L/s), gives the final equation

$$r_{FeS_2} = \frac{N\upsilon(R^* + 1)}{(15R^* + 14) m_{FeS_2}} \quad (11)$$

After the reaction solution passes through the packed bed, the value of R^* should decrease due to the reaction. Therefore, the value of R^* in eq 11 should be the average between the inlet and the outlet of the packed bed.

The analytical method used to determine the ferric ion and total iron concentrations utilized the 1.10 phenanthroline colorimetric method given by Vogel (1978). A spectrophotometer was used for this analysis.

Results and Discussion

Effect of Ferric/Ferrous Ratio and Total Iron Concentration. The flow rate of the lixiviant through the packed bed was varied to ensure that the experimental reaction condition was kinetically controlled rather than mass-transfer-limited. The oxidation rate was found to be 0.164×10^{-3} kg/m^2/s at a flow rate of 1.11 mL/s and 0.161×10^{-3} kg/m^2/s at a flow rate of 3.33 mL/s for the Sargent-Welch pyrite. The difference in the rates is well within the error generated by the experimental procedure. The reaction conditions were considered not to be mass-transfer-limited. Mathews and Robins (1972) reported activation energies of 79.55 and 92.11 kJ/mol for two different pyrite samples using a $Fe_2(SO_4)_3$–H_2SO_4 system. King and Perlmutter (1977) obtained an activation energy of 52.75 kJ/mol using a $FeCl_3$–HCl system. These activation energies indicate a kinetically limited reaction.

The kinetics of heterogenous catalytic reactions have been successfully represented by Hougen and Watson (1943, 1947) and Yang and Hougen (1950) who analyzed a number of possible reaction mechanisms based on the Langmuir–Hinshelwood adsorption isotherm. The rate expressions obtained are valid when purely chemical phenomena determine the observed conversion rates. This particular approach assumes that the driving force for the reaction is the surface concentrations of the adsorbed species, rather than the concentrations of the species present in the fluid phase. In this manner, the rate expression developed from the rate data can be used for design purposes well beyond the conditions under which the experimental data were obtained.

The experimental results obtained in this study were found to fit the Hougen–Watson "dual-site" rate expression model by Hill (1977) and Smith et al. (1958) for total Fe(III) and total Fe(II) adsorption. According to such a model, Fe(III) and Fe(II) ions compete for adsorption on dual active sites on the pyrite surface. The adsorption of a Fe(III) ion on two adjacent active sites leads to the formation of an activated complex of Fe(III) ion on the surface. This activated complex of Fe(III) ion is decomposed to yield an activated complex of Fe(II) ion by electron transfer and acting concurrently with this process is the continual decomposition of the activated complex of Fe(II) ion and desorption of Fe(II) ions back into solution. The overall process can be represented by the following reactions.

$$Fe^{III} + 2C_\sigma \overset{K_1}{\rightleftharpoons} Fe^{III}{*}\cdot 2C_\sigma \tag{12}$$

$$Fe^{II} + 2C_\sigma \overset{K_2}{\rightleftharpoons} Fe^{II}{*}\cdot 2C_\sigma \tag{13}$$

$$Fe^{III}{*}\cdot 2C_\sigma + e^- \overset{K_3}{\rightleftharpoons} Fe^{II}{*}\cdot 2C_\sigma \quad K_3 = k_{3f}/k_{3r} \tag{14}$$

$$Fe^{II}{*}\cdot 2C_\sigma \rightleftarrows Fe^{II} + 2C_\sigma \tag{15}$$

If the fraction of the active site adsorbing Fe(III) and Fe(II) is denoted by $\theta_{Fe(III)}$ and $\theta_{Fe(II)}$, respectively (where an active site adsorbs a half Fe(III) ion or a half Fe(II) ion), the fraction that is bare will be $[1 - \theta_{Fe(III)} - \theta_{Fe(II)}]$.

When the Hougen–Watson concepts are used, the rate-limiting step is the chemical reaction rate on the surface, and the equilibrium is established with respect to adsorption of all species. Thus, we have

$$K_1 = \frac{\theta_{Fe(III)}{}^2}{Fe(III)[1 - \theta_{Fe(III)} - \theta_{Fe(II)}]} \tag{16}$$

$$K_2 = \frac{\theta_{Fe(II)}{}^2}{Fe(II)[1 - \theta_{Fe(III)} - \theta_{Fe(II)}]} \tag{17}$$

where the concentrations of the chemical species are used instead of the activity. For a certain species, the changes in the activity a_j and molality m_j when the pyrite is oxidized are related by

$$da_j = d(\gamma_j m_j) \tag{18}$$

$$\frac{da_j}{dm_j} = \gamma_j + m_j \frac{d\gamma_j}{dm_j} \tag{19}$$

In a multicomponent electrolyte solution, the concentration of a single species will not have much influence on the ionic strength I and hence

$$\frac{d\gamma_j}{dm_j} = \frac{d\gamma_j}{dI}\frac{dI}{dm_j} \simeq 0 \tag{20}$$

Thus,

$$\frac{da_j}{dm_j} = \gamma_j = \frac{a_j}{m_j} \tag{21}$$

$$\frac{da_j}{a_j} = \frac{dm_j}{m_j} \tag{22}$$

$$d \ln a_j = d \ln m_j \tag{23}$$

Under this condition, the activity a_j is equal to the molality m_j.

The rate of pyrite oxidation according to eq 14 is given by

$$r_{FeS_2} = k_{3f}\theta_{Fe(III)} - k_{3r}\theta_{Fe(II)} \tag{24}$$

The following rate equation can be derived from (16), (17), and (24):

$$r_{FeS_2} = \frac{k_{3f}K_1^{1/2} - k_{3f}K_2^{1/2}/K_3[Fe(II)/Fe(III)]^{1/2}}{1/[Fe(III)]^{1/2} + K_1^{1/2} + K_2^{1/2}[Fe(II)/Fe(III)]^{1/2}} \tag{25}$$

Equation 25 can be rewritten by substituting R^* for the ferric/ferrous ratio and combining the constants to give

$$r_{FeS} = \frac{\kappa_1 - \kappa_2(1/R^*)^{1/2}}{1/[Fe(III)]^{1/2} + \kappa_3 + \kappa_4(1/R^*)^{1/2}} \tag{26}$$

where $\kappa_1 = \kappa_{3f}K_1^{1/2}$, $\kappa_2 = \kappa_{3f}(K_2/K_3)^{1/2}$, $\kappa_3 = K_1^{1/2}$, and $\kappa_4 = K_2^{1/2}$.

At high emf values (0.700 V), $1/R^*$ goes to zero, hence, eq 25 simplifies to the linear expression

$$\frac{1}{FeS_2} = \frac{1}{\kappa_1[Fe(III)]^{1/2}} + \frac{\kappa_3}{\kappa_1} \tag{27}$$

A plot of $1/r_{FeS_2}$ vs. $1/[Fe(III)]^{1/2}$ yields a straight line with a slope of $1/\kappa_1$ and an intercept of κ_3/κ_1 as shown in Figure 1. Least-squares analysis of these plots resulted in a slope of 0.162, intercept of 0.642, and a correlation coefficient R^2 of 0.999 for the Sargent-Welch pyrite and a slope of 0.164, an intercept of 0.629, and a correlation coefficient R^2 of 0.98 for the H. Wilhelm pyrite. Potentiostatic data,

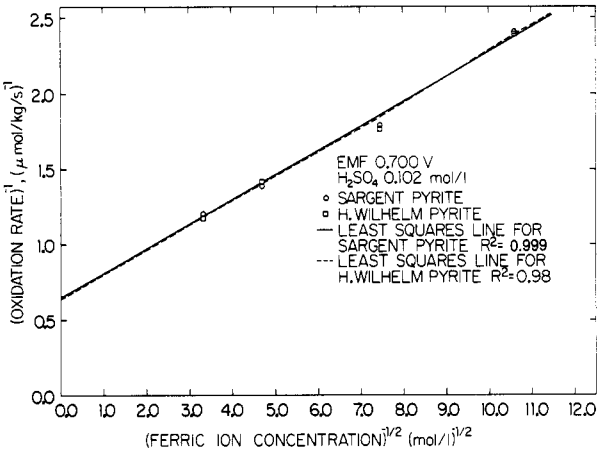

Figure 1. Plot of the reciprocal oxidation rate of pyrite vs. (ferric ion concentration)$^{-1/2}$ at high redox potential of the solution.

Table I. Calculated Values of the Constants in Equation 26[a]

pyrite ore	1	2	3	4	source
Sargent-Welch	22.0	7.30	3.70	73.0	this work
H. Wilhelm	21.3	7.10	3.50	88.4	this work
Museum-grade	20	6.7	1.4	300	Smith and Shumate, 1970
Sulfur Ball No. 2	165	55	2.3	70	Smith and Shumate, 1970

[a] Note: r (rate) in units of mmol of FeS_2 oxidized/h/kg of sample; the concentration of Fe(III) in unit of mol/L.

obtained by Smith and Shumate (1970) using a pyrite anode and a saturated KCl reference electrode, indicated that κ_2 was approximately equal to $\kappa_1/3.0$. This result was used to evaluate κ_2. Equation 26 was used to obtain a value for κ_4. By using experimental rate data and the estimated values for κ_1, κ_2, and κ_3, it was possible to determine κ_4 values for each experimental run. These κ_4 values were then averaged to obtain the best estimated for κ_4. These estimates for the four constants are then incorporated into eq 26 to give

$$r_{FeS_2} = \frac{6.10 - 2.03(1/R^*)^{1/2}}{1/[\mathrm{Fe(III)}]^{1/2} + 3.84 + 91.1(1/R^*)^{1/2}} \quad (28)$$

with the rate and the ferric ion concentration expressed in units of μmol/kg/s and mol/L, respectively, for the H. Wilhelm pyrite.

The estimates for the constants and a comparison of the experimental results with those of Smith and Shumate (1970) are given in Table I.

Comparisons of the experimental rate of reaction with the rate predicted by using eq 26 are shown in Figures 2 and 3. The experimental data are in good agreement with the predicted results.

Figure 2 shows that the rate of reaction of pyrite increases with increasing emf and total iron concentration. Figure 3 shows that as the emf of the solution is increased to the point where all the iron is ferric, the rate becomes constant. The experimental results can be fitted by several other curves and are in good agreement with Sasmojo (1969) and Smith and Shumate (1970) and further support the adsorption mechanism and model used to represent the dissolution reaction. In addition, the four constants given in Table I are similar in magnitude to those obtained for the Museum-grade pyrite used by Smith and Shumate (1970).

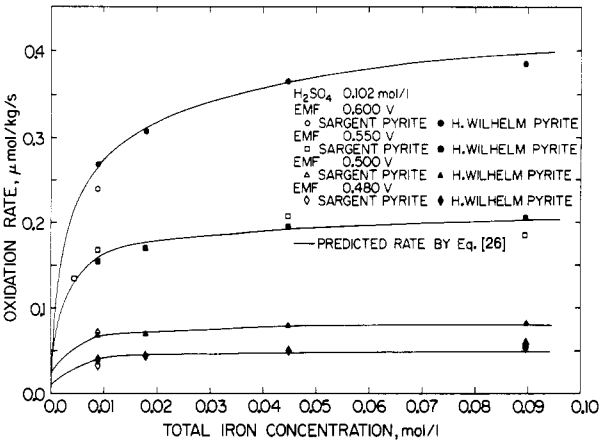

Figure 2. Effect of the total iron concentration of the leaching solution on the oxidation rate of pyrite.

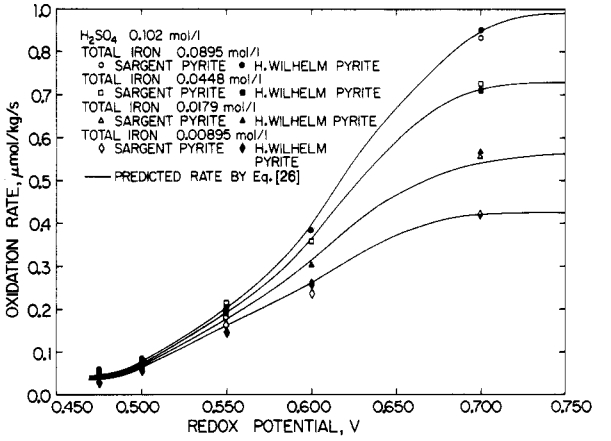

Figure 3. Effect of the redox potential of the leaching solution on the oxidation rate of pyrite.

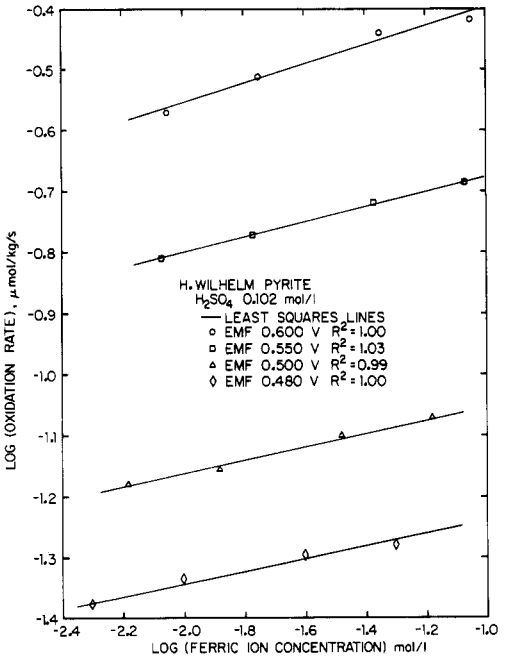

Figure 4. Plot of log (oxidation rate) vs. log (ferric ion concentration of leaching solution).

An increase in the total iron concentration will increase the rate, since at constant ferric/ferrous ratio an increase in total iron concentration would be accompanied by a corresponding increase in ferric ion concentration.

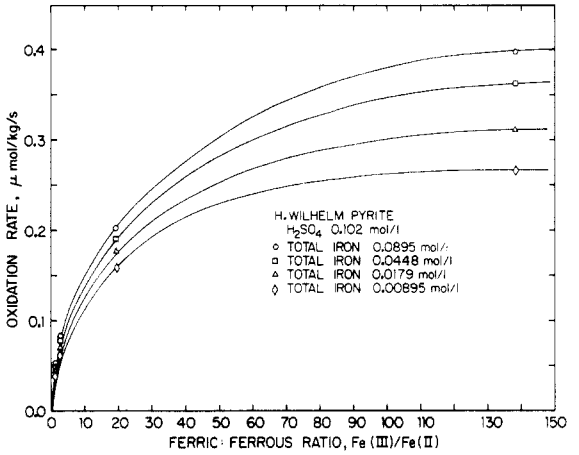

Figure 5. Effect of the ferric/ferrous concentrations of the leaching solution on the oxidation rate of pyrite.

The experimentally determined rate was found to depend on the ferric ion concentration according to the expression

$$r(\mu\text{mol/kg/s}) = k_{\text{Fe(III)}}[\text{Fe(III)}]^b \qquad (29)$$

As shown in Figure 4, the values of b are 0.0962, 0.107, 0.122, and 0.157 and the values of the rate constant $k_{\text{Fe(III)}}$ are 0.071, 0.112, 0.280, and 0.574 at an emf of 0.480, 0.500, 0.550, and 0.600 V, respectively. The values of b increase slowly from 0.0962 to 0.157 with an increase in emf from 0.480 to 0.600 V. The rate constants also increase with an increase in emf.

The effect of the ferric/ferrous ratio on the oxidation is shown in Figure 5. The rate increases with increasing ferric/ferrous ratio irrespective of the total iron concentration in solution.

Effect of Sulfate and Sulfate Concentrations on Oxidation Rate. Previous work by Garrels and Thompson (1960), Smith and Shumate (1970), Sasmojo (1969), and Mathews and Robins (1972) reported on the effect of acid and sulfate concentrations on the oxidation rate of pyrite. The effects of varying the sulfate concentration were discussed to some extent by Sasmojo (1969) and Smith and Shumate (1970). Both reported a decrease in the oxidation rate of pyrite with increasing sulfate concentration added as Na_2SO_4 and/or H_2SO_4.

A detailed analysis of the effects of sulfate concentration relative to changes in the species composition of the leaching solution has never been reported. In this study, the rate of pyrite oxidation was correlated with the various species assumed to be present in the leaching solution. The species composition of the leaching solution was computed from the initial analytical concentration of $Fe_2(SO_4)_3$, $FeSO_4$, H_2SO_4, and/or Na_2SO_4 by using a set of nonlinear equations in the partial equilibrium model developed by Helgeson (1968) and applied to leaching of chalcopyrite by Liddell (1977) and Liddell and Bautista (1980, 1981, 1981). The effect of the sulfate anion or the effect of the acid strength on the oxidation kinetics of pyrite is evaluated in detail.

Plots of log (rate) vs. log (total sulfate concentration) shown in Figure 6 give two straight lines when Na_2SO_4 concentration or H_2SO_4 concentration is varied. The total sulfate concentration dependence of the oxidation rate is given by eq 30 where $k_{SO_4^{2-}}$ is the rate constant derived from the intercept and c is the slope given in Figure 6.

$$r_{FeS_2} = k_{SO_4^{2-}}(SO_4^{2-})^c \qquad (30)$$

The values of c are −0.456 and −0.872, and the values of

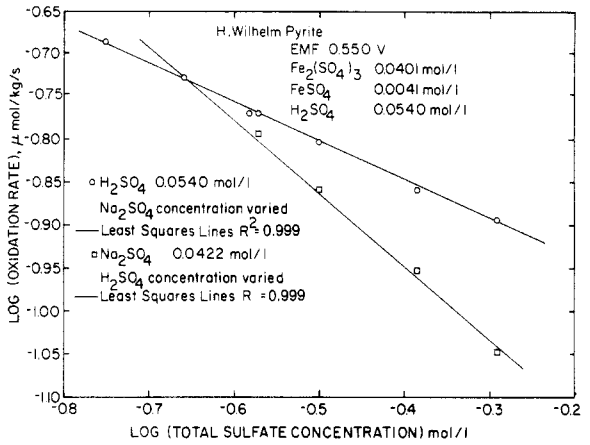

Figure 6. Plot of log (oxidation rate of pyrite) vs. log (total sulfate concentration of the leaching solution).

Table II. Chemical Species in an Aqueous Solution of $Fe_2(SO_4)_3$, $FeSO_4$, H_2SO_4, and Na_2SO_4: Unknown Concentrations in the Partial Equilibrium Model Equation

H_+	$Fe(SO_4)_2^-$	$FeOH^{2+}$	$FeHSO_4^+$
SO_4^{2-}	$FeHSO_4^{2+}$	$Fe(OH)_2^+$	Na^+
HSO_4^-	Fe^{2+}	$Fe(OH)_2^{4+}$	$NaSO_4^-$
Fe^{3+}	$FeSO_4$	$FeSO_4$	

Table III. Simultaneous Equilibrium Reaction in a Solution Containing $Fe_2(SO_4)_3$, $FeSO_4$, H_2SO_4, and Na_2SO_4

$H^+ + SO_4^{2-} \rightleftharpoons HSO_4^-$	(31)
$Fe^{3+} + H_2O \rightleftharpoons FeOH^{2+} + H^+$	(32)
$FeOH^{2+} + H_2O \rightleftharpoons Fe(OH)_2^+ + H^+$	(33)
$2FeOH^{2+} \rightleftharpoons Fe_2(OH)_2^{4+}$	(34)
$Fe^{3+} + SO_4^{2-} \rightleftharpoons FeSO_4^+$	(35)
$FeSO_4^+ + SO_4^{2-} \rightleftharpoons Fe(SO_4)_2^-$	(36)
$Fe^{3+} + HSO_4^- \rightleftharpoons FeHSO_4^{2+}$	(37)
$Fe^{2+} + SO_4^{2-} \rightleftharpoons FeSO_4$	(38)
$Fe^{2+} + HSO_4^- \rightleftharpoons FeHSO_4^+$	(39)
$Na^+ + SO_4^{2-} \rightleftharpoons NaSO_4^-$	(40)

the rate constant $k_{SO_4^{2-}}$ are 0.0933 and 0.351 at a H_2SO_4 concentration of 0.0540 mol/L and a Na_2SO_4 concentration of 0.0422 mol/L, respectively, with the rate in units of μmol/kg/s and the sulfate concentration in units of mol/L.

Figure 6 shows that the rate of oxidation decreases continuously with increasing sulfate concentration, regardless of whether the sulfate addition is with Na_2SO_4 or H_2SO_4. However, for a given total sulfate concentration, the solution where the H_2SO_4 concentration was varied exhibited a faster decrease in oxidation rate compared to where the Na_2SO_4 concentration was varied.

The outline of the procedure used to determine the species composition in the leaching solution is as follows. The details of the calculational method have previously been reported (Liddell, 1977; Liddell and Bautista, 1980, 1981, 1981).

The species whose concentrations have been taken as unknowns in the model are listed in Table II. The chemical reactions occurring in the solution are shown in Table III. For each of the 10 reactions given in Table III, there is a mass action equation. The apparent equilibrium constants determined for high ionic strength solutions given by Smith and Martell (1976) have been used. The 10 mass action equations are given in Table IV.

From the concentration of $Fe_2(SO_4)_3$, $FeSO_4$, H_2SO_4, and Na_2SO_4, material balance equations can be written for Fe(III), Fe(II), Na^+, and SO_4^{2-}. A charge balance is also written for the system. These balance equations are shown in Table V. When all the reactions are equilibrium reactions as in this case, the number of equations exactly matches the number of unknowns. There are 15 nonlinear

Table IV. Mass Action Equations and Apparent Equilibrium Constants for a Solution Containing $Fe_2(SO_4)_3$, $FeSO_4$, H_2SO_4, and Na_2SO_4

	K_{app}	ionic strength	ref	equation
$0 = K_{1,app} - (m_{H^+}m_{SO_4^{2-}}/m_{HSO_4^-}$	1.23×10^{-1}	3.0	Liddell and Bautista, 1980	41
$0 = K_{2,app} - [m_{Fe^{3+}}/(m_{H^+}m_{FeOH^{2+}})]$	9.35×10^{2}	3.0	Liddell and Bautista, 1980	42
$0 = K_{3,app} - [m_{FeOH^{2+}}/(m_{H^+}m_{Fe(OH)_2^+})]$	1.95×10^{3}	3.0	Liddell and Bautista, 1980	43
$0 = K_{4,app} - (m_{FeOH^{2+}}{}^2/m_{Fe_2(OH)_2^{4+}})$	6.62×10^{-4}	3.0	Liddell and Bautista, 1980	44
$0 = K_{5,app} - (m_{SO_4^{2-}}m_{Fe^{3+}}/m_{FeSO_4^+})$	1.18×10^{-2}	3.0	Liddell and Bautista, 1980	45
$0 = K_{6,app} - (m_{SO_4^{2-}}m_{FeSO_4^+}/m_{Fe(SO_4)_2^-})$	6.62×10^{-1}	3.0	Liddell and Bautista, 1980	46
$0 = K_{7,app} - (m_{HSO_4^-}m_{Fe^{3+}}/m_{FeHSO_4^{2+}})$	2.50×10^{-1}	2.67	Liddell and Bautista, 1980	47
$0 = K_{8,app} - (m_{SO_4^{2-}}m_{Fe_2^{2+}}/m_{FeSO_4})$	4.85×10^{-1}	3.0	Liddell and Bautista, 1980; Liddell, 1977	48
$0 = K_{9,app} - (m_{HSO_4^-}m_{Fe_2^{2+}}/m_{FeHSO_4^+})$	5.15×10^{-1}	4.0	Wells and Salam, 1968	49
$0 = K_{10,app} - (m_{SO_4^{2-}}m_{Na^+}/m_{NaSO_4^-})$	2.00×10^{-1}	3.0	Liddell and Bautista, 1980	50

Table V. Balance Equations for a Solution Containing $Fe_2(SO_4)_3$, $FeSO_4$, H_2SO_4, and Na_2SO_4

Fe(III) balance

$$0 = 2C_{Fe_2(SO_4)_3} - m_{Fe^{3+}} - m_{FeOH^{2+}} - m_{Fe(OH)_2^+} - 2m_{Fe_2(OH)_2^{4+}} - m_{FeSO_4^+} - m_{Fe(SO_4)_2^-} - m_{FeHSO_4^{2+}} \quad (51)$$

Fe(II) balance

$$0 = C_{FeSO_4} - m_{Fe^{2+}} - m_{FeSO_4} - m_{FeHSO_4^+} \quad (52)$$

sodium balance

$$0 = 2C_{Na_2SO_4} - m_{Na^+} - m_{NaSO_4^-} \quad (53)$$

sulfate balance

$$0 = 3C_{Fe_2(SO_4)_3} + C_{FeSO_4} + C_{Na_2SO_4} + C_{H_2SO_4} - m_{SO_4^{2-}} - m_{FeHSO_4^-} - m_{FeSO_4^+} - m_{Fe(SO_4)_2^-} - m_{FeHSO_4^{2+}} - m_{FeSO_4^+} - m_{FeHSO_4^+} - m_{NaSO_4^-} \quad (54)$$

charge balance

$$0 = m_{H^+} - 2m_{SO_4^{2-}} - m_{HSO_4^-} + 3m_{Fe^{3+}} + 2m_{FeOH^{2+}} + m_{Fe(OH)_2^+} - 4m_{Fe_2(OH)_2^{4+}} + m_{FeSO_4^+} - m_{Fe(SO_4)_2^-} + 2m_{FeHSO_4^{2+}} + 2m_{Fe^{2+}} + m_{FeHSO_4^+} + m_{Na^+} - m_{NaSO_4^-} \quad (55)$$

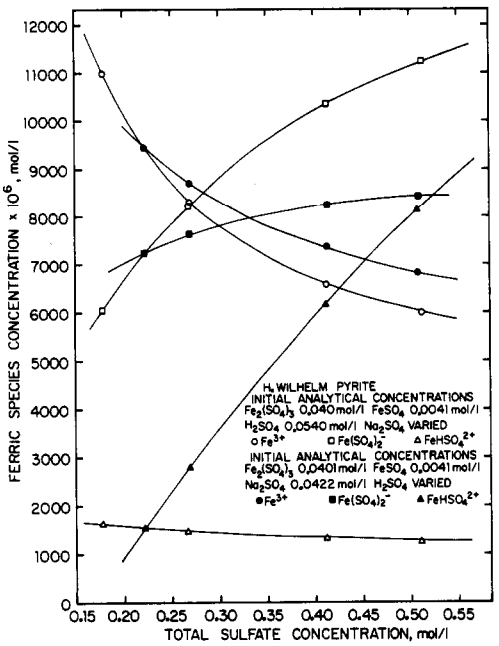

Figure 7. Changes in the concentration of Fe^{3+}, $Fe(SO_4)_2^-$, and $FeHSO_4^{2+}$ when the total sulfate concentration is changed by addition of either Na_2SO_4 or H_2SO_4.

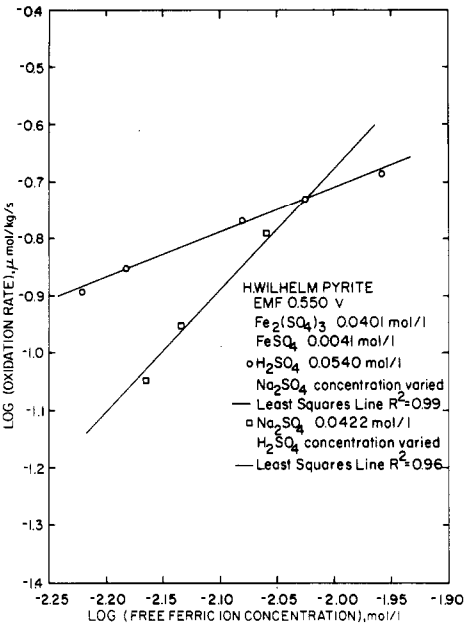

Figure 8. Plot of log (oxidation rate) vs. log (free ferric ion concentration of leaching solution).

equations and 15 unknown species concentrations.

The numerical method used to solve eq 41–55 is the Newton–Raphson iteration technique given by Carnahan et al. (1969). The computations involved in the Gauss–Jordan elimination and back-substitution procedure are given in detail by Liddell (1977). The four analytical concentrations appearing in the mass balances are specified. To begin the iteration procedure, initial guesses for the values of each of the 15 unknowns must be made. This iterative process was repeated until either (1) the convergence criteria were met or (2) the number of iterations reached a preset maximum value. In the latter case, new initial guesses must be made.

The calculated species compositions in the leaching solution are given in Tables VI and VII. The data show that under acidic leaching condition, the most abundant ferric ion species are $FeSO_4^+$, $Fe(SO_4)_2^-$, and free ferric ion. The $FeHSO_4^{2+}$ ion present is less than 3% of the $FeSO_4^+$, and the amount of hydrated ferric ions present is insignificant. The data show that any increase in the sulfate concentration in the leaching solution either by Na_2SO_4 or H_2SO_4 additions results in changes in the Fe(III) species present in the solution. The free ferric ions decrease and the $Fe(SO_4)_2^-$ ions increase with increasing sulfate concentration and the $FeSO_4^+$ concentration remained constant. The addition of sulfate as H_2SO_4 increases the $FeHSO_4^{2+}$ concentration as shown in Table VII. Changes in the concentrations of free Fe^{3+}, $Fe(SO_4)_2^-$, and $FeHSO_4^{2+}$ species with an increase in the sulfate concentration either by Na_2SO_4 or by H_2SO_4 additions are shown in Figure 7. It is evident that the decrease in the rate of pyrite oxidation with increasing sulfate concentration is a function of the ferric species present in the solution.

Table VI. Concentration of the Different Species in Solution and the Oxidation Rate of H. Wilhelm Pyrite Sample at Different Initial Concentration of Na_2SO_4 (Initial Analytical Concentration: $Fe_2(SO_4)_3$, 0.0401; $FeSO_4$, 0.0041; H_2SO_4, 0.0540 mol/L)

Na_2SO_4, mol/L	0.0000	0.0422	0.0899	0.2340	0.3320
SO_4^{2-}, mol/L	0.1784	0.2206	0.2683	0.4124	0.5104
H^+, mol/L × 10^6	69360	65319	62029	56029	53640
SO_4^{2-}, mol/L × 10^6	65660	77389	88092	110580	120980
HSO_4^-, mol/L × 10^6	37026	41097	44425	50371	52760
Fe^{3+}, mol/L × 10^6	11005	9420	8301	6581	6001
$FeOH^{2+}$, mol/L × 10^6	170	154	143	126	120
$Fe(OH)_2^+$, mol/L × 10^6	1	1	1	1	1
$Fe_2(OH)_2^{4+}$, mol/L × 10^6	43	36	31	24	22
$FeSO_4^+$, mol/L × 10^6	61234	61782	61971	61676	61522
$Fe(SO_4)_2^-$, mol/L × 10^6	6073	7222	8246	10302	11243
$FeHSO_4^{2+}$, mol/L × 106	1630	1549	1475	1326	1266
Fe^{2+}, mol/L × 106	3396	3308	3234	3093	3033
$FeSO_4$mol/L × 10^6	460	528	587	705	757
$FeHSO_4^+$, mol/L × 10^6	244	264	279	302	311
Na^+, mol/L × 10^6	0	60854	124820	301370	413740
$NaSO_4^-$, mol/L × 10^6	0	23547	54979	166630	250260
pH_{calcd}	1.159	1.185	1.207	1.252	1.271
pH_{exptl}	1.327	1.288	1.291	1.322	1.322
r_{exptl}, μmol/kg/s	0.206	0.187	0.171	0.139	0.128
r_{calcd}, μmol/kg/s	0.217	0.188	0.168	0.135	0.124

Table VII. Concentration of the Different Species in Solution and the Oxidation Rate of H. Wilhelm Pyrite Samples at Different Initial Concentration of H_2SO_4 (Initial Analytical Concentration: $Fe_2(SO_4)_3$, 0.0401; $FeSO_4$, 0.0041; Na_2SO_4, 0.0422 mol/L)

Na_2SO_4, mol/L	0.0540	0.1020	0.2460	0.3420
SO_4^{2-}, mol/L	0.2206	0.2686	0.4126	0.5086
H^+, mol/L × 10^6	65319	119330	275320	375300
SO_4^{2-}, mol/L × 10^6	77389	82946	93595	98063
HSO_4^-, mol/L × 10^6	41097	80471	209500	299210
Fe^{3+}, mol/L × 10^6	9420	8686	7361	6831
$FeOH^{2+}$, mol/L × 10^6	154	78	28	19
$Fe(OH)_2^+$, mol/L × 10^6	1	0	0	0
$Fe(OH)_2^{4+}$, mol/L × 10^6	36	9	1	1
$FeSO_4^+$, mol/L × 10^6	61782	60986	58385	56765
$Fe(SO_4)_2^-$, mol/L × 10^6	7222	7641	8255	8409
$FeHSO_4^{2+}$, mol/L × 10^6	1549	2796	6168	8175
Fe^{2+}, mol/L × 10^6	3308	3089	2563	2300
$FeSO_4$, mol/L × 10^6	528	528	495	465
$FeHSO_4^+$, mol/L × 10^6	264	483	1042	1336
Na^+, mol/L × 10^6	60854	59658	57494	56632
$NaSO_4^-$, mol/L × 10^6	23547	24742	26906	27768
pH_{calcd}	1.185	0.923	0.560	0.426
pH_{exptl}	1.288	1.009	0.782	0.663
r_{exptl}, μmol/kg/s	0.187	0.161	0.112	0.0897
r_{calcd}, μmol/kg/s	0.188	0.159	0.109	0.0883

The oxidation rate of pyrite was observed to decrease with decreasing free ferric ion concentration. This is a result of the increase in sulfate concentration. Plots of log (rate) vs. log (free ferric ion concentration) shown in Figure 8 give two straight lines when Na_2SO_4 and H_2SO_4 concentrations are varied. The free ferric ion concentration dependence of the oxidation rate is given by eq 56 where $k_{Fe^{3+}}$ is the rate constant derived from the intercept and d is the slope in Figure 8. The values of d are 0.792 and

$$r_{FeS_2} = k_{Fe^{3+}}(Fe^{3+})^d \quad (56)$$

2.16, and the values of the rate constant $k_{Fe^{3+}}$ are 7.45 and 13.4 at a H_2SO_4 concentration of 0.0540 mol/L and Na_2SO_4 concentration of 0.0422 mol/L, respectively, with the rate in units of μmol/kg/s and the free ferric ion concentration in units of mol/L.

The complexed ferric sulfate ions are large and are not readily adsorbed on the surface of pyrite, thereby hindering the adsorption process. These complexes ions also have a reduced positive charge relative to free Fe^{3+} ions because of the negative charges of the complexed sulfate anions surrounding the ferric ion, causing an inhibition of electron transfer. On the basis of the above conditions, the decrease in the free ferric ions and the increase in the complexed ferric ions with increasing sulfate concentration result in the decrease in the rate of pyrite oxidation. This would indicate that only the free ferric ions are active in the oxidation reaction with pyrite.

The decrease in ferric concentration is greater when the sulfate is added as Na_2SO_4 instead of H_2SO_4. This is shown in Figure 7. However, the decrease in the rate of pyrite oxidation is faster with the addition of H_2SO_4 than with the addition of Na_2SO_4 as shown in Figures 6 and 8. This is a result of the difference in the changes in concentrations of $FeHSO_4^+$ as shown in Figures 7 and 9 under both conditions. The results show that at a given total sulfate concentration, the resulting leaching solution with increasing H_2SO_4 concentration exhibited much larger increases in $FeHSO_4^{2+}$ and HSO_4^- concentration than with Na_2SO_4. This in turn reduces the pyrite oxidation rate. This may be the result of the formation of HSO_4^-–Fe^{3+} complexes which compete for adsorption with Fe^{3+} and Fe^{2+} ions on the reactive sites of the pyrite surface, thus reducing the number of reactive sites for the leaching reaction to take place. Leaching under constant iron sulfate concentration and continuous addition of H_2SO_4 could

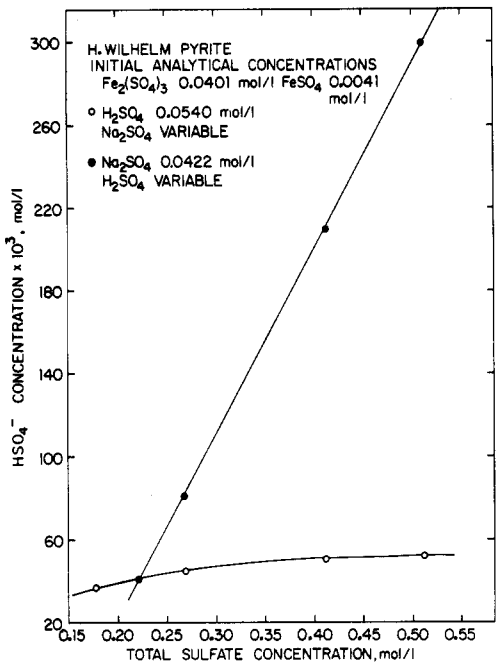

Figure 9. Changes in the concentration of HSO_4^- when the total sulfate concentration is changed by addition of either Na_2SO_4 or H_2SO_4.

result in the increased concentration of HSO_4^-, thereby resulting in the increased concentration of $FeHSO_4^{2+}$ and slowing down of the leaching rate.

On the basis of the above discussion, the other possible mechanism of the oxidation reaction of pyrite can be postulated, following the Hougen–Watson simple adsorption–irreversible reaction model of Hill (1977) and Smith et al. (1958). The rate can be expressed in terms of the concentrations of the adsorbed species which take part in the reactions instead of just being dependent on the total Fe(III) ions and total Fe(II) ions concentrations. It is assumed that all the species that take part in the various reactions are adsorbed on the surface sites of pyrite. An adsorbed ferric ion reacts with a vacant site to form an activated complex and then oxidizes the pyrite (and as mentioned in the electrochemical reaction of pyrite, pyrite itself has a potential difference) to form the activated complex of ferrous ion and elemental sulfur. The elemental sulfur produced is not thermodynamically stable, and in the experimental condition of this work, the excess ferric ions in the solution will react with this sulfur to form the sulfate ion (Garrels and Thompson, 1960). The sulfate ions produced can then associate with the H^+ ion from the acidic solution to form HSO_4^-. The HSO_4^- ion formed subsequently reacts with the ferric ion to form the complexed $FeHSO_4^{2+}$ ion which will compete for adsorption with the Fe^{3+} and Fe^{2+} ions. The more H_2SO_4 added, the more $FeHSO_4^{2+}$ ions are formed. Therefore the decrease in pyrite oxidation is faster with the addition of H_2SO_4 than with Na_2SO_4. This means that the decrease in rate with increasing addition of H_2SO_4 is not only due to the decrease in free ferric ion concentration but also due to the inhibitory effect of the complex $FeHSO_4^{2+}$ ion. The overall process can be represented by the following reaction:

$$Fe^{3+} + C_\sigma \overset{K_1'}{\rightleftharpoons} Fe^{3+}\text{*}\cdot C_\sigma \quad (57)$$

$$Fe^{2+} + C_\sigma \overset{K_2'}{\rightleftharpoons} Fe^{2+}\text{*}\cdot C_\sigma \quad (58)$$

$$FeHSO_4^{2+} + C_\sigma \overset{K_a'}{\rightleftharpoons} FeHSO_4^{2+}\text{*}\cdot C_\sigma \quad (59)$$

$$Fe^{3+}\text{*}\cdot C_\sigma + {}^1/_2FeS_2 + {}^1/_2C_\sigma \overset{k'}{\rightleftharpoons} {}^3/_2Fe^{2+}\text{*}\cdot C_\sigma + S^0 \quad (60)$$

$$S^0 + 6Fe^{3+} + 4H_2O \rightleftarrows SO_4^{2+} + 6Fe^{2+} + 8H^+ \quad (61)$$

$$H^+ + SO_4^{2-} \rightleftarrows HSO_4^- \quad (31)$$

$$Fe^{3+} + HSO_4^- \rightleftarrows FeHSO_4^{2+} \quad (37)$$

Equation 60 is basically an electron-transfer step. It should be slow, since the electron transfer must take place through a layer of sulfur pyrite. Equation 60 can be rewritten as

$$Fe^{3+}\text{*}\cdot C_\sigma + {}^1/_2FeS_2 \xrightarrow[\text{transfer}]{\text{electron}} Fe^{2+}\text{*}\cdot C_\sigma + {}^1/_2(FeS_2)^{2+} \quad (60a)$$

$${}^1/_2(FeS_2)^{2+} + {}^1/_2C_\sigma \xrightarrow[\text{transfer}]{\text{atom}} {}^1/_2Fe^{2+}\text{*}\cdot C_\sigma + S^0 \quad (60b)$$

In this mechanism, eq 60b is the rate-determining step and represents the passage of Fe^{2+} throught the sulfur film. If there is a sulfur film with a steady-state thickness, it would be much slower than the electron transfer.

If the fraction of the reactive site adsorbing the Fe^{3+}, Fe^{2+}, and $FeHSO_4^{2+}$ is denoted by $\theta_{Fe^{3+}}$, $\theta_{Fe^{2+}}$, and $\theta_{FeHSO_4^{2+}}$, respectively, the fraction that is bare will be $[1 - \theta_{Fe^{3+}} - \theta_{Fe^{2+}} - \theta_{FeHSO_4^{2+}}]$. Thus, the rate of pyrite oxidation according to eq 60 is given by

$$r_{FeS} = k'\theta_{Fe^{3+}}(1 - \theta_{Fe^{3+}} - \theta_{Fe^{2+}} - \theta_{FeHSO_4^{2+}})^{1/2} \quad (62)$$

Substituting into eq 62 the equilibrium constants and concentrations of the species (Fe^{3+}), (Fe^{2+}), and $(FeHSO_4^{2+})$ in eq 57, 58, and 59 and rearranging give

$$r_{FeS_2} = \frac{k'K_1'(Fe^{3+})}{[1 + K_1'(Fe^{3+}) + K_2'(Fe^{2+}) + K_a'(FeHSO_4^{2+})]^{3/2}} \quad (63)$$

From eq 47

$$(FeHSO_4^{2+}) = \frac{(HSO_4^-)(Fe^{3+})}{K_{7,app}} \quad (64)$$

Substituting into eq 63 the concentration of $FeHSO_4^{2+}$ given by eq 66 and combining the constants give

$$r_{FeS_2} = \frac{k'K_1'(Fe^{3+})}{[1 + K_1'(Fe^{3+}) + K_2'(Fe^{2+}) + K_3'(Fe^{3+})(HSO_4^-)]^{3/2}} \quad (65)$$

where $K_3' = K_a'/K_{7,app}$.

Equation 65 can also be rewritten

$$r_{FeS_2} = (k'K_1')/\{(Fe^{3+})^{1/2}[1/(Fe^{3+}) + K_1' + K_2'(Fe^{2+})/(Fe^{3+}) + K_3'(HSO_4^-)]^{3/2}\} \quad (66)$$

Four simultaneous equations are set up replacing the r_{FeS_2}, (Fe^{3+}), (Fe^{2+}) and (HSO_4^-) in eq 65 with the experimental data given in Table VII. The four unknowns are the constants k', K_1', K_2', and K_3'. Solving simultaneously these nonlinear equations gives the approximate values of the constants. The values of k', K_1', K_2', K_3', and K_a' are 7.86, 3.00, 1.00, 220, and 55.0, respectively. These estimates are then incorporated into eq 65 to give

$$r_{FeS_2} = \frac{23.6(Fe^{3+})}{[1 + 3.00(Fe^{3+}) + 1.00(Fe^{2+}) + 220(Fe^{3+})(HSO_4^-)]^{3/2}} \quad (67)$$

with the rate and the ion concentrations expressed in units

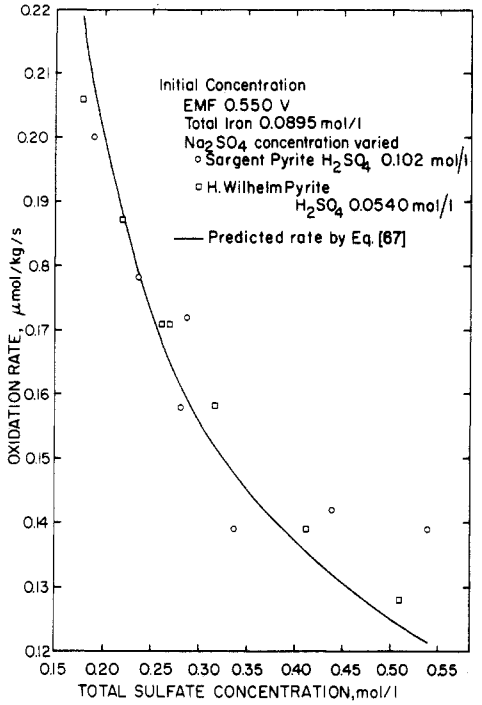

Figure 10. Comparison of the experimental rate with the rate predicted by using eq 67.

of μmol/kg/s and mol/L, respectively.

A comparison of the experimental rate of the reaction with the rate predicted by using eq 67 is shown in Figure 10. The experimental data are in agreement with the predicted data.

The comparison of the experimental rate with the rates calculated from eq 67 is given in Tables VI and VII.

Conclusion

The kinetic study on the dissolution of pyrite was found to be influenced by the Fe(III), Fe(II), sulfate, and acid concentrations. The oxidation reaction at constant acid concentration could be represented by a Hougen–Watson dual-site adsorption model with the electron-transfer reaction being the rate-limiting step. The derived rate expression

$$r_{FeS_2} = \frac{\kappa_1 - \kappa_2 - [Fe(II)/Fe(III)]^{1/2}}{1/([Fe(III)]^{1/2} + \kappa_3 + \kappa_4 [Fe(II)/Fe(III)]^{1/2})} \quad (26)$$

is in good agreement with the experimental results for two pyrite specimens from different localities. At constant acid concentration, the Fe(III) and Fe(II) species competed for the reactive sites on the pyrite surface.

The dependence of the rate on the ferric ion concentration could also be expressed by eq 29 with the values of the rate constant $k_{Fe(III)}$ and the exponent b increasing with greater ferric/ferrous ratio.

An increase in the total sulfate concentration by the addition of either Na_2SO_4 or H_2SO_4 was found to decrease the oxidation rate. At a given potential, the dependence of the rate on the total sulfate concentration was given by eq 30.

Determining the composition of all the species in the lixiviant solution by using the partial equilibrium model showed that the increased sulfate concentration in the leaching solution resulted in a decrease in the free Fe^{3+} ions and an increase in some of the complexed ferric ion species. The dependence of the rate on the free ferric ion concentration was given by eq 56.

The large complexed ferric ion species have a lower positive charge density relative to the free Fe^{3+} ions, hence inhibiting electron transfer and thereby limiting adsorption.

Increasing the sulfuric acid concentration in the leaching solution resulted in an increase in the concentration of $FeHSO_4^{2+}$ complex ions. The HSO_4^- ions formed from the ferric bisulfate species compete for the active sites, with ferric ions thereby reducing the number of sites available for oxidation of pyrite. This in turn leads to a reduction in the leaching rate.

On the basis of the above discussion, the oxidation rate of pyrite at different sulfate concentration is a function of the free ferric, free ferrous, and bisulfate ions (or HSO_4^-–Fe^{3+} complex ions). This could be represented by a Hougen–Watson simple adsorption irreversible reaction model and is given by eq 65.

The experimental rate data obtained for two pyrite samples from different localities were in agreement with the derived rate.

Finally, eq 26 best represents the oxidation rate of the pyrite under constant acid concentration. In the case where the sulfate concentration is varied, eq 65 is best in representing the oxidation rate of the pyrite.

Acknowledgment

This research was supported in part by the Mining and Mineral Resources Research Institute and by the Ames Laboratory, USDOE, in the form of graduate assistantships to C.C.A. and by the Department of Metal Materials, Chengdu University of Science and Technology, Chengdu, Sichuan, Peoples Republic of China, for a sabbatical leave to C.Q.Z. The experimental work on the rate of oxidation of the H. Wilhelm pyrite sample was supported by the U.S. Department of Energy, under contract No. W-7405-ENG-82, by the Director for Energy Research, Office of Basic Energy Science, Chemical Sciences program. The experimental work on the rate of oxidation of the Sargent-Welch pyrite sample was supported by the U.S. Bureau of Mines, Department of Interior under grant no. 65106002.

Nomenclature

a_j = activity of chemical species
C = concentration of vacant active sites on the pyrite surface
Fe^{II}_T = initial total ferrous ion concentration
Fe^{III}_T = initial total ferric ion concentration
$Fe^{II}{*}\cdot 2C_\sigma$ = activated complex of Fe(II) ions
$Fe^{III}{*}\cdot 2C_\sigma$ = activated complex of Fe(III) ions
$Fe^{3+}{*}\cdot C_\sigma$ = activated complex of Fe^{3+} ions
$Fe^{2+}{*}\cdot C_\sigma$ = activated complex of Fe^{2+} ions
$FeHSO_4^{2+}{*}\cdot C_\sigma$ = activated complex of $FeHSO_4^{2+}$
I = ionic strength
K_1 = adsorption equilibrium constant for Fe(III) ions
K_2 = adsorption equilibrium constant for Fe(II) ions
K_3 = equilibrium constant of electron-transfer reaction $k_3 = k_{3f}/k_{3r}$
k_{3f} = rate constant for forward electron-transfer reaction
k_{3r} = rate constant for reverse electron-transfer reaction
$k_{Fe(III)}$ = rate constant of eq 29
$k_{Fe^{3+}}$ = rate constant of eq 56
$k_{SO_4^{2-}}$ = rate constant of eq 30
K_1' = adsorption equilibrium constant for Fe^{3+} ions
K_2' = adsorption equilibrium constant for Fe^{2+} ions
K_a' = adsorption equilibrium constant for $FeHSO_4^{2+}$ ions
k' = rate constant of eq 60
κ_1 = constant in eq 26, $\kappa_1 = K_{3f} K_1^{1/2}$
κ_2 = constant in eq 26, $\kappa_2 = k_{3f} K_2^{1/2}/K_3^{1/2}$
κ_3 = constant in eq 26, $\kappa_3 = K_1^{1/2}$
κ_4 = constant in eq 26, $\kappa_4 = K_2^{1/2}$
M_{FeS_2} = mass of pyrite sample, kg

m_j = concentration of chemical species
N = normality of titrant
R^* = ratio of ferric to ferrous
r_{FeS_2} = rate of oxidation, μmol/s/kg
t = time required for pyrite oxidation, s
v = rate of titrant addition, L/s
V_T = initial volume of leaching solution, L
x = amount of ferrous ion oxidized to ferric ion to maintain constant R^*

Greek Letters

$\theta_{Fe(II)}$ = fraction of active site adsorbing Fe(II) ions
$\theta_{Fe(III)}$ = fraction of active site adsorbing Fe(III) ions
$\theta_{Fe^{2+}}$ = fraction of active site adsorbing Fe^{2+} ions
$\theta_{Fe^{3+}}$ = fraction of active site adsorbing Fe^{3+} ions
$\theta_{FeHSO_4^{2+}}$ = fraction of active site adsorbing $FeHSO_4^{2+}$ ions
γ_j = activity coefficient of chemical species

Registry No. $Fe_2(SO_4)_3$, 10028-22-5; pyrite, 1309-36-0.

Literature Cited

Allen, C. C. M.S. Thesis, Iowa State University, Ames, 1982.
Ammou-Chokroum, M. *Bull. Miner.* **1979**, *102*, 708.
Bave, A. V.; Orlov, A. I. *Izv. Vyssh. Uchebn. Zaved., Tsvetn. Metall.* **1975**, *5*, 18.
Biegler, T.; Rand, D. A. J.; Woods, R. J. *J. Electroanal. Chem. Interfacial Electrochem.* **1975**, *60*, 151.
Braley, S. A. Research Summary Report on Fellowship, No. 326B to Mellon Institute, 1953.
Bryner, L. C.; Jameson, A. K. *Appl. Microbiol.* **1958**, *6*, 281-287.
Carnahan, B.; Luther, H. A.; Wilkes, J. O. "Applied Numerical Methods"; Wiley: New York, 1969; pp 270-273, 319-323.
Corrick, J. D.; Sutton, J. A. U.S. Bureau of Mines, RI 6714, Washington, DC, 1965.
Garrles, R. M.; Thompson, M. E. *Am. J. Sci. 258-A*, **1960**, 57-67.
Helgeson, H. C. *Geochim. Cosmochim. Acta* **1968**, *32*, 853-877.
Hill, Charles, G., Jr. "An Introduction to Chemical Engineering Kinetics and Reactor Design"; Wiley: New York, 1977; pp 167-190.
Hougen, O. A.; Watson, K. M "Chemical Processes Principles"; Chapman and Hall: London, 1947; Vol. III.
Hougen, O. A.; Watson, K. M. *Ind. Eng. Chem.* **1943**, *35*, 529-541.
King, W. E.; Perlmutter, D. D. *AIChE J.* **1977**, *23* (5), 679-685.
Liddell, K. C. Ph.D. Thesis, Iowa State University, Ames, 1977.
Liddell, K. C.; Bautista, R. G. In "Thermodynamics of Aqueous Systems with Industrial Applications"; Newman, S. A., Ed.; American Chemical Society: Washington, DC, 1980; ACS Symp. Ser. No. 133, pp 741-755.
Liddell, K. C.; Bautista, R. G. In "Process and Fundamental Consideration of Selected Hydrometallurgical System"; Kuhn, M. C., Ed.; Society of Mining Engineers of AIME: New York, 1981; pp 334-344.
Liddell, K. C.; Bautista, R. G. *Metall. Trans. B* **1981**, *12B*, pp 627-637.
Lowson, R. I. *Chem. Rev.* **1982**, *82* (5), pp 461-497.
Lowson, R. T. 6th RACT National Convention, Surfers Paradise, Australia, Nov 5-10, 1979.
Masuko, N.; Hisamatsu, Y. *Nippon Kogyo Kaishi* **1967**, *83*, 153.
Mathews, C. T.; Robins, R. G. *Aust. Chem. Eng.* **1972**, *No. 9*, pp 21-25.
Sapieszko, R. S.; Patel, R. C.; Matijeric, E. *J. Phys. Chem.* **1977**, *81*, 1061-1068.
Sasmojo, S. Ph.D. Thesis, The Ohio State University, Columbus, 1969.
Schaeffer, W. I.; Holbert, P. E.; Umbreit, W. W. *J. Bacteriol.* **1963**, *85*, 137.
Smith, E. E.; Shumate, K. S. Water Pollution Control Research Series, 14010 fps 02/70. U.S. Dept. of the Interior, Washington, DC, 1970.
Smith, E. E.; Svanks, K.; Shumate, K. S. Paper Presented at the 2nd Symposium on Coal Mine Drainage Research, Pittsburgh, PA, May, 1958.
Smith, R. M.; Martell, A. E. "Critical Stability Constants"; Plenum Press: New York, 1976; Vol. 4, pp 79-81.
Stokes, H. N. *U.S. Geol. Surv. Bull.* **1970**, *186*, 11.
Sutton, J. A.; Corrick, J. D. *Min. Eng. (Littleton, Colo.)* **1963**, *15* (6), 37-40.
Sutton, J. A.; Corrick, J. D. U.S. Bureau of Mines, Washington, DC, RI #6423, 1964.
Tveter, E. C.; McQuiston, F. W., Jr. In "Froth Flotation"; Fuerstenau, D. W., Ed.; AIME: New York, 1962; 50th Anniversary Volume.
Vogel, A. I. "A Textbook of Quantitative Inorganic Analysis, Including Elementary Instrumental Analysis", 4th ed.; Longman: New York, 1978.
Wells, C. F.; Salam, M. A. *J. Chem. Soc. A* **1968**, 308-315.
Woodcock, J. T. *Proc., Australas. Inst. Min. Metall.* **1961**, *198*, 47.
Yang, K.; Hougen, O. A. *Chem. Eng. Prog.* **1950**, *46*, 148-157.

Received for review February 13, 1984
Revised manuscript received June 21, 1985
Accepted July 24, 1985

COMMUNICATIONS

Gas-Phase Reactions of Chloroform and 1,1,2-Trichloroethane with Hydrogen in a Tubular Flow Reactor

Reactions of hydrogen with chloroform and 1,1,2-trichloroethane were studied in a tubular reactor at a pressure of 1 atm and in the temperatures range of 550–1100 °C. Reagent loss and product formation were monitored by using an on-line gas chromatograph, where batch samples were analyzed by GC/mass spectrometry. The major products of reactions of hydrogen with chloroform and 1,1,2-trichloroethane above 850 °C were observed as the thermodynamically stable species HCl, CH_4, and carbon (solid). The more stable chlorinated byproducts, chloromethane and vinyl chloride, were also observed at low concentrations, and higher temperatures were required for the subsequent decomposition of these products. Complete destruction of the parent reagent, chloroform and 1,1,2-trichloroethane, was observed at temperatures near 700 °C with residence times slightly over 1 s. The activation energies were determined to be 48.6 kcal/mol for reaction of chloroform with hydrogen and 48.8 kcal/mol for reaction of 1,1,2-trichloroethane with hydrogen.

The principal method for destruction of toxic or carcingenic species such as chlorocarbon solvents, PCB's, DDT, dioxins, etc., is to incinerate them in a reactor where the materials have a 2-s residence time at a temperature of 1200 °C in the presence of excess oxygen or where 99.99% conversion is demonstrated (Manson and Unget, 1979). The carbon contained in the reagent species is supposed to be totally oxidized to CO_2. This technique may destroy all the initial parent species, but reaction products are not all converted to carbon dioxide, as these combustion facilities are run in an 0_2-rich environment where there is no stable and desirable end adduct for the chlorine. Chlorine oxides and Cl_2 are not acceptable end products for discharge to the atmosphere nor are they formed in a selective or quantitative manner for complete collection or neutralization. One preferred chloride product might be hydrogen chloride, which could be quantitatively neutralized or collected. The relatively low content of hydrogen-containing species in the reactor or inlet mixtures combined with excess oxygen, unfortunately, precludes the stoichiometric formation of HCl in many incinerations. This is readily demonstrated by the fact that

0196-4305/86/1125-0317$01.50/0